Automated Detection of Bolus Arrival and Initiation of Data Acquisition in Fast, Three-dimensional, Gadolinium-enhanced MR Angiography[1]

Thomas K. F. Foo, PhD
Manojkumar Saranathan, MSc
Martin R. Prince, MD, PhD
Thomas L. Chenevert, PhD

Automatic triggering of magnetic resonance (MR) angiography with detection of a contrast material bolus was evaluated. Signal intensity changes with time were tracked in a prescribed tracking or monitoring volume by a parallel signal processing unit that automatically started data acquisition once user-defined thresholds were exceeded. This technique, referred to as MR Smartprep, was reliable and avoided the inconsistencies of manual timing.

Index terms: Magnetic resonance (MR), contrast enhancement, 9*.12917,[2] 9*.129412, 9*.12942, 9*.12943 • Magnetic resonance (MR), three-dimensional, 9*.12917 • Magnetic resonance (MR), vascular studies, 9*.129412, 9*.12942

Radiology 1997; 203:275–280

MAGNETIC resonance (MR) angiography with the infusion of contrast material has been demonstrated to be a robust imaging technique (1–8). The basic principle is the use of a fast three-dimensional (3D) gradient-echo, preferably radio-frequency phase-spoiled pulse sequence for better stationary spin contrast, with repetition times (TRs) of 4–9 msec and infusion of a high-relaxivity (R1) contrast material timed such that the arterial phase of the bolus infusion coincides with the acquisition of data from the center of k space in the region of interest. Timing the arrival of the contrast material bolus to the acquisition of the central k-space lines is critical to the success of this method (7–9).

Timing is even more imperative in short-TR images (10–30-second breath holds), for which there is the possibility of completely missing the contrast material bolus. With a short image acquisition time, there is a much smaller margin of error in timing the start of the bolus infusion relative to the start of data acquisition. Starting the data acquisition too early reduces the effectiveness of the contrast material bolus, because the contrast material bolus has not completely filled the arterial structures within the entire image field of view (FOV). Conversely, if data acquisition occurs too late, the contrast material may have passed and there may be filling of the venous structures, which complicates the image analysis. Because the transit time of a contrast material bolus from the infusion site to the imaged region of the body varies with heart rate, cardiac output, age, and severity of the vascular abnormality, accurate prediction of this parameter is difficult.

We present a technique that we refer to as MR Smartprep (GE Medical Systems, Milwaukee, Wis), which uses a tracking pulse sequence to continuously monitor the MR signal from a user-prescribed volume of interest. As the signal from this region increases because of the arrival of contrast material (such as gadolinium-based contrast material or any suitable contrast material that substantially reduces the T1 of blood) in the arterial structures, the pulse sequence controller checks to determine if the signal intensity amplitude threshold values are exceeded. Once the measured signal intensity exceeds the threshold values, the pulse sequence controller automatically begins data acquisition. To maximize the image contrast at this point, the low spatial frequency data in the phase-encoding direction are acquired first, that is, in centric order.

The proposed technique has an added feature of continuously providing feedback to the imaging operator on the different stages of the acquisition process. Indication is given on when the contrast material bolus infusion may be started, on detection of the bolus (which signals the patient to begin a breath hold), on the playing out of dummy radio-frequency excitations, and on the start of data acquisition.

Materials and Methods

All experiments were performed with a 1.5-T Signa MR imaging system (GE Medical Systems, Milwaukee, Wis). The block diagram of Figure 1 provides a description of the hardware architecture that facilitates real-time monitoring of the MR signal intensity in a prescribed tracking volume. A TMS320C30 (Texas Instruments, Dallas, Tex) digital signal processing unit has direct access to the MR time-domain data from the receiver channel. It has two-way communication with the pulse sequence controller, known as the intersequence process generator, by means of a dual-ported shared random-access memory, or RAM, structure. In this manner, the intersequence process generator is able to use the additional vector processing capabilities of the digital signal processing chip in the signal processing unit for rapid data processing and pass the result back to the primary pulse sequence controller. This setup allows the pulse sequence controller to monitor the signal intensity changes in a prescribed tracking volume and to modify waveform instructions on a real-time basis before the next TR.

Two different pulse sequences were used in the proposed technique: a tracking sequence and an imaging sequence. In the tracking sequence, a 90°–180° spin echo with no phase-encoding gradients was used (Fig 2). Orthogonal section-selective gradients for the 90° and 180° radio-frequency pulses defined a rectangular volume in the patient (Fig 3). Only spins from within this volume were refocused with the 180° radio-frequency pulse and returned a spin echo. Spatial localization in the third dimension was facilitated by offsetting the receiver frequency and by using the bandwidth-limiting function of the anti-aliasing filter in the receiver channel.

Thus, a precise 3D volume was defined with the tracking sequence. For some applications in which the tracking volume must be placed over the aortic arch or carotid artery, a much smaller tracking volume, especially in the read-out direction, is required. To attain tracking volume lengths of less than 20 cm in the read-out direction, a fast Fourier transform was applied to the frequency-encoded data.

Flow compensation was imple-

[1] From the Applied Science Laboratory, GE Medical Systems, Bldg 10, Rm B1D-161, 10 Center Dr, MSC 1061, Bethesda, MD 20892-1061 (T.K.F.F.); the Department of Biomedical Engineering, University of Washington, Seattle (S.M.); and the Department of Radiology, University of Michigan, Ann Arbor (M.R.P., T.L.C.). Received September 19, 1996; revision requested November 5; revision received December 16; accepted December 23. **Address reprint requests to** T.K.F.F.

[2] 9* indicates general vascular involvement.

mented in the read-out direction to maximize the signal-to-noise ratio of flowing spins in the tracking volume. To minimize the tracking-sequence echo time (8–10 msec), a default volume of 4 × 4 × 20 cm was used. The tracking-sequence TR of 20 msec also defined the temporal resolution for tracking the signal intensity changes. A short TR for the spin-echo tracking sequence was used to ensure complete saturation of all stationary (background) tissue. Only spins with an extremely short T1 relaxation time, such as contrast material–laden blood, will return an appreciable MR signal intensity increase.

The tracking volume can be graphically prescribed in an oblique orientation to maximize the fraction of flowing spins to stationary tissue in the monitoring volume, as shown in Figure 4. The size of the tracking volume was also adjusted to maximize the sensitivity to changes in the tracking signal intensity from the contrast material bolus. There is less of a signal intensity increase when the tracking volume encompasses only a small fraction of a primary artery.

The proposed automated bolus detection technique can be divided into four phases or segments. The first was an initial dummy radio-frequency excitation phase of 2–3 seconds to allow the spins to attain a dynamic equilibrium state. This was followed by a baseline acquisition phase of 14–16 seconds. The purpose of the baseline segment was to acquire statistics on the mean signal intensity and standard deviation (variance) of the MR signal intensity in the tracking volume to set the detection thresholds. During the first two phases, the MR system timer was stopped. At the end of the second (baseline) phase, the system timer was reactivated, which indicated to the imager operator that the third, tracking phase had started. Contrast material was then administered (15–40 mL of gadodiamide [Omniscan; Nycomed, Oslo, Norway]).

During the tracking phase of imaging, the magnitude of the time-domain echo signal was integrated over the total analog-to-digital converter sampling time if the tracking FOV was 20 cm or larger. For smaller tracking FOVs, only the pixels that corresponded to the smaller FOV were integrated in the image domain after performance of a fast Fourier transform on the time-domain data. Although data can be generated for every tracking-sequence TR (of 20 msec), every 20 data points were averaged together to provide better statistics, which gave an effective tracking temporal resolution of 400 msec per output point.

The flow chart for the proposed technique is shown in Figure 5. After the

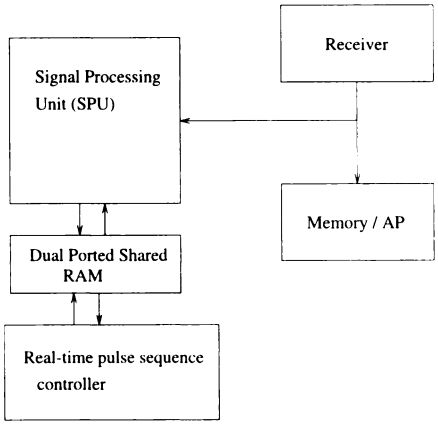

Figure 1. Block diagram illustrates the hardware architecture that enables the real-time pulse sequence controller to decide on the next course of action. *AP* = anteroposterior, *RAM* = random-access memory.

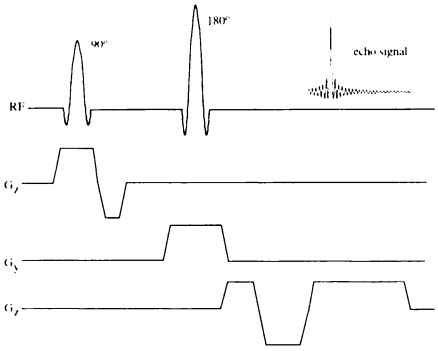

Figure 2. Tracking or monitoring pulse-sequence diagram. The orthogonal section-selective gradients in the z and y directions select out a rectangular volume along the x direction. Flow compensation and a fractional echo readout are used to maximize the echo signal intensity from flowing spins. *RF* = radio frequency.

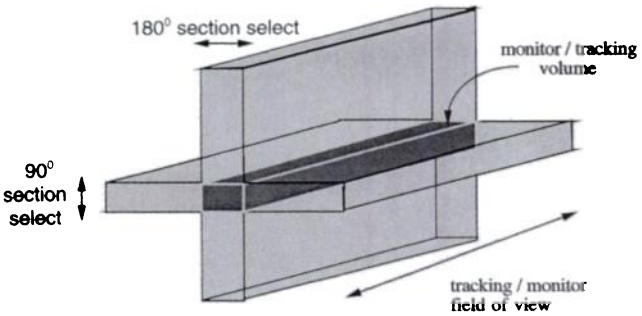

Figure 3. Diagram of the tracking volume generated by the orthogonal section-selection gradients for the 90° and 180° radio-frequency pulses. The length of the rectangular volume (tracking FOV) is defined by the receiver filter bandwidth and has a minimum acquired tracking FOV of 20 cm. For a smaller tracking FOV, the echo signal is Fourier transformed and the magnitude signal intensity is summed over the number of pixels that correspond to a smaller tracking FOV.

baseline segment, the first and second thresholds were set. The first threshold (S_1) was set at

$$S_1 = \bar{s} + n \cdot \sigma, \quad (1)$$

where $\bar{s}$ is the mean signal intensity, n is the number of standard deviations, and σ is standard deviation.

The purpose of the first threshold was to ensure that signal intensity variations due to respiration did not prematurely trigger the start of data acquisition. The first threshold value was typically set to 3 standard deviations. For the second threshold level, a 20% increase in the signal intensity from the mean was used for all images when more than 20 mL of gadodiamide was administered. For studies in which at most 20 mL of contrast material was administered, there was a reduced T1 relaxivity effect and, thus, a smaller signal intensity amplitude increase. Accordingly, the second threshold level was reduced to 15%. This second threshold (S_2) was user selectable and was given as $S_2 = \bar{s} \cdot (1.0 + m)$, where m is the percentage of increase in the mean signal intensity.

Once a signal intensity change beyond the threshold levels was detected, the intersequence process generator switched from the 20-msec spin-echo tracking sequence to the 3D radio-frequency phase-spoiled gradient-echo imaging sequence (fourth phase) with a TR of 4–9 msec, depending on the gradient performance of the MR system and the image prescription. At this point, the system timer was again halted to indicate to the technologist the time at which the bolus was detected. Note that the imaging volume was prescribed independently of the tracking volume. Two section-encoding loops (of 16 steps each, independent of the number of section partitions prescribed and at a TR of 4–9 msec) with data acquisition turned off were used to establish a dynamic equilibrium state for the imaging sequence. This ini-

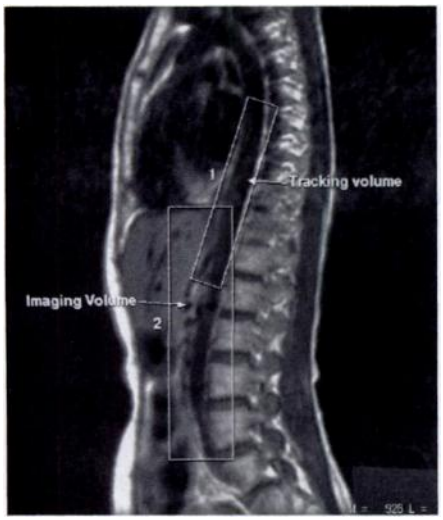

Figure 4. Diagram illustrates the positioning of the tracking volume for a coronal 3D imaging volume on a sagittal scout image. To ensure that the tracking volume has maximum sensitivity to the passage of the contrast material, it is placed along the section of the descending aorta as close to the imaging volume as possible. The ability to prescribe an oblique tracking volume and to adjust its size to fit the primary arterial structure ensures that a higher percentage of signal intensity change is noted as the contrast material shortens the T1 of blood. If the tracking volume is too large, the large fraction of stationary tissue will mask any signal intensity increases because of the contrast material in the vasculature.

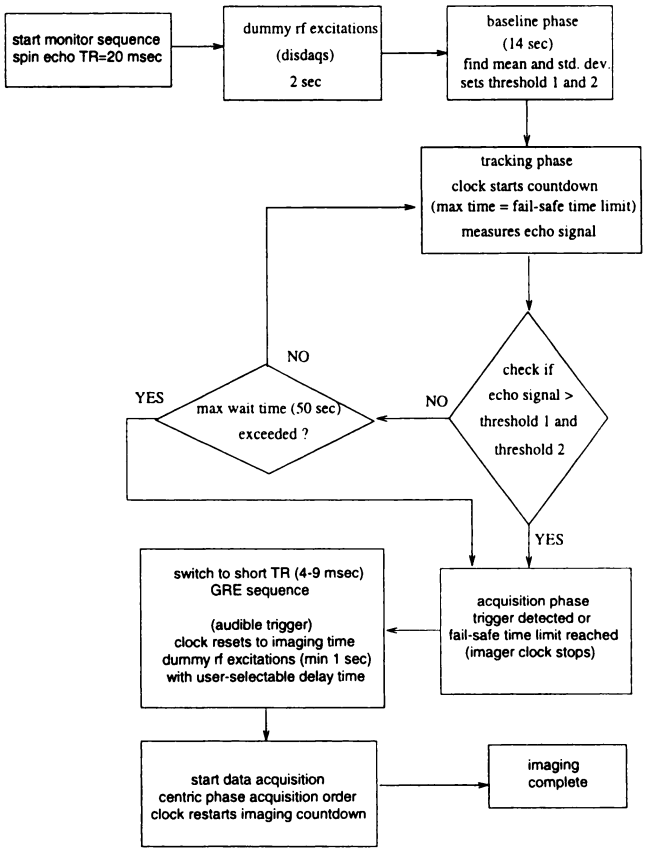

Figure 5. Flow chart of the MR Smartprep technique. *disdaqs* = dummy radio-frequency excitations, *GRE* = gradient echo, *max* = maximum, *min* = minimum, *rf* = radio frequency, *std. dev.* = standard deviation.

tial delay could be extended to allow time for collateral arterial structures to fill in. This delay was adjusted 1–5 seconds for different anatomic regions.

The switch from the 20-msec spin-echo pulse sequence to the short-TR, 3D gradient-echo sequence generated a noticeable audible signal. This signaled the patient, who had been coached before imaging, to begin breath holding. For abdominal imaging, a 1–5-second delay was determined to both allow the collateral arterial vasculature to fill-in and to provide sufficient time for the patient to take in a deep breath and then suspend breathing. At the start of image data acquisition, the clock was reset to the total imaging time and restarted. To maximize vessel contrast, data acquisition was structured such that the outer phase-encoding loop was acquired in a centric-view acquisition order (10), while the inner section-encoding loop was acquired in a sequential order.

In the event that a trigger was not detected, a fail-safe time limit was implemented. The pulse sequence controller continued monitoring for a signal intensity increase up to a user-defined fail-safe time limit. This limit was set at 30–50 seconds after the baseline acquisition period. The fail-safe limit is an important component, because patient motion may cause the desired anatomic tracking region in the patient to be shifted away from the physical location of the tracking volume, which prevents the detection of the contrast material bolus passage. This fail-safe strategy was designed to prevent the tracking phase from continuing indefinitely.

Image acquisition was performed with a fast, 3D, radio-frequency phase-spoiled, gradient-echo pulse sequence with a short (4–9-msec) TR and a 44° flip angle. Image FOV varied from 20 cm to 48 cm, with 2.0–3.0-mm sections and 32–40 section partitions, depending on the patient size and the anatomic region to be covered. This resulted in sequence echo times of 1.2–2.4 msec. Initial studies were performed on a 10-mT/m, 17-T · m^{-1} · sec^{-1} slew rate MR system. An upgraded gradient performance package was later installed and used for all remaining studies (22-mT/m gradient amplitude and 77-T · m^{-1} · sec^{-1} slew rate). Acquisition matrices varied from 256 × 128 to 256 × 192. With these imaging parameters, total imaging time was 20–30 seconds.

Studies were performed in patients according to institutional review board guidelines and with informed consent. At the time this article was written, approximately 75 patients had been examined with this technique. The statistical significance of the differences between automated bolus-detection MR angiographic and manually timed MR angiographic images will be the subject of a future presentation and is beyond the scope of this article. A contrast material infusion rate of approximately 2 mL/sec was used in all experiments, and contrast material was delivered manually. After each study, the tracking volume signal intensity–time curve was written out to a data file to be viewed at a later time.

Results

The change in signal intensity amplitude with time during the tracking period in abdominal MR angiography is shown in Figure 6. Steady state is achieved during the first 2 seconds, followed by a modulation in the signal intensity before the administration of 40 mL of gadodiamide. The modulation in the signal intensity was due to respiratory motion and was ignored by using a first threshold level of 3 standard deviations from the mean (n = 3 in Eq [1]). A valid trigger is reported by the signal processing unit only if the signal intensity exceeded both the first threshold

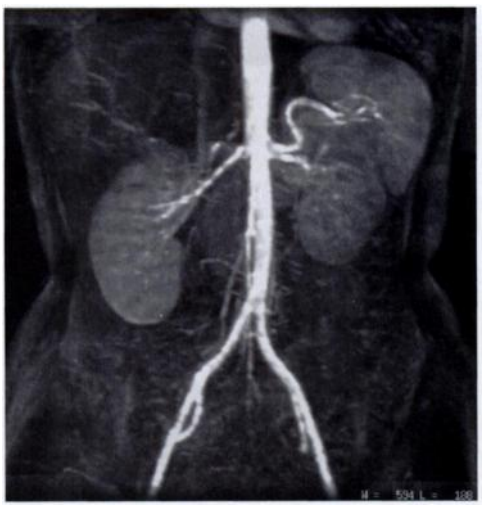

7a. 7b. 8.

Figures 7, 8. **(7)** Maximum intensity projection images (9.4/2.4 [TR msec/echo time msec], 44° flip angle, 28-cm FOV, ±16 kHz bandwidth, 2.5-mm sections, body coil, 39-second imaging time) obtained in a 43-year-old female patient during a 28-section coronal automated bolus-detection acquisition; images correspond to the data in Figure 6. **(a)** Triggered 3D image, obtained with the start of data acquisition delayed 5 seconds after the detection of a signal intensity increase beyond the threshold values. The patient was asked to breath hold when the gradient rhythm changed after the trigger was detected. **(b)** Delayed 3D image acquired 4 minutes after the first image. Note that venous structures are more apparent and that the vascular signal intensity is markedly reduced. **(8)** Automated bolus-detection triggered MR angiographic image (10.1/2.8, 45° flip angle, 24-cm FOV, 32 1.5-mm-thick sections, 256 × 160 matrix, ±16 kHz bandwidth, one signal acquired) obtained in a male patient with bilateral carotid stenoses. The tracking volume was placed at the level of the aortic arch, and a 2-second delay after the trigger was used. The threshold levels were set at 3 standard deviations from the mean and a 20% signal intensity increase.

and a second threshold 20% above the mean.

The corresponding maximum intensity projection image from this acquisition, obtained by using a delay after the trigger of 5 seconds, is shown in Figure 7a. This image exhibits increased signal intensity in the arterial structures and minimal signal intensity in the venous structures, which demonstrates that the pulse sequence controller was able to intelligently track the arrival of the contrast material bolus and initiate the start of data acquisition at the correct time. Had the pulse sequence controller been in error, there would be minimal or no signal intensity enhancement (if data acquisition started before the arrival of the contrast material bolus) or enhancement of both arterial and venous structures, as shown in the delayed acquisition in Figure 7b.

The automated bolus-detection technique was also used successfully in regions other than the abdomen, which include the thoracic aorta and carotid arteries (Fig 8). By placing the tracking volume in either the common carotid artery or the aortic arch and by using a minimal (1-second) delay after the trigger, the contrast material in the arterial phase can be easily imaged for MR angiograms of the head and neck. Because of the fast blood circulation times in the head, some enhancement of the jugular veins was also observed. The corresponding signal intensity–time plot of Figure 8 is shown in Figure 9. The data plot shows a steady rise in signal intensity amplitude as the contrast material bolus passes through the aortic arch, which triggers the start of data acquisition at about 26 seconds from the end of the baseline phase.

Discussion

Other techniques that have been used for contrast material infusion MR angiography include use of an average transit time to delay the start of acquisition from administration of the contrast material bolus. This is not a foolproof solution, because placement at the center of k space at the requisite time delay from the point of contrast material administration depends on how precisely the MR technologist is able to synchronize the start of the bolus infusion to the start of imaging. In addition, there will be patients who do not conform to the average flow profile, which makes such manual timing methods yield unpredictable results.

Methods to more accurately determine the contrast material bolus transit time by performing test bolus imaging, where the imaging region of interest is imaged repeatedly with a fast gradient-echo sequence, have their limitations. By using a test bolus, the image operator will have to identify the image with the optimal contrast material inflow characteristics to determine the appropriate transit time. This removes the patient-to-patient variability, but the problem of correctly synchronizing the administration of the contrast material bolus to the start of imaging remains. Furthermore, the 2–4 mL of contrast material used for the test bolus leads to an increase in the signal intensity of the tissue parenchyma, which contributes to a less than optimal stationary spin

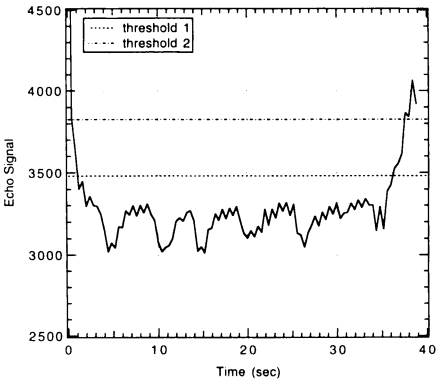

Figure 6. Signal intensity–time plot for an abdominal MR angiographic study performed in a patient after the administration of 40 mL of gadodiamide. In this example, a 4 × 5 × 20-cm volume was placed over the descending aorta. The threshold levels of 3 standard deviations from the mean and a 20% rise in signal intensity over the mean are shown. Note the approach to the steady state and the modulation in the signal intensity change due to respiration. Signal intensity tracking is enabled after the first 16 seconds to permit time for dummy radiofrequency excitations (2 seconds) and the baseline acquisition phase (14 seconds). The trigger was detected at 37.6 seconds from the start of the tracking segment.

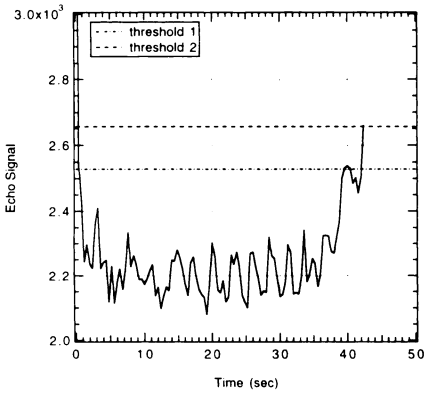

9.

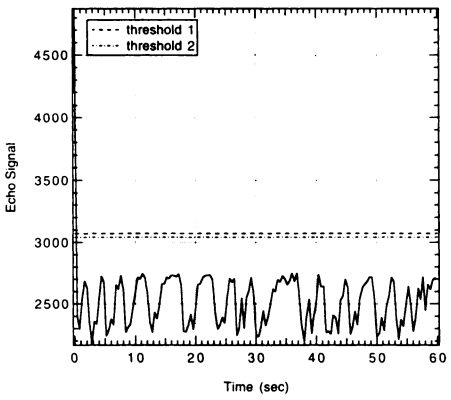

10.

Figures 9, 10. **(9)** Signal intensity–time plot of a carotid MR angiographic study performed in a patient after the administration of 40 mL of gadodiamide; image corresponds to data in Figure 7. For this study, the tracking volume was placed over the aortic arch. The pulse sequence controller detected a valid trigger at the threshold values (3 standard deviations, 20% signal intensity increase) about 29 seconds after the start of the tracking phase. **(10)** Signal intensity–time plot of an automated bolus-detection triggered study in which the pulse sequence controller failed to detect a signal intensity increase. As shown in the plot, there is no indication of any signal intensity changes apart from those due to respiration. For this study, a maximum fail-safe limit of 45 seconds was used. Even though the tracking algorithm did not detect the passage of contrast material, the pulse sequence controller automatically started data acquisition at the end of the fail-safe period. The failure in this study was probably due to patient movement that shifted the aorta from the prescribed tracking volume. This is evidenced by the nearly constant mean signal intensity and periodic signal intensity variation.

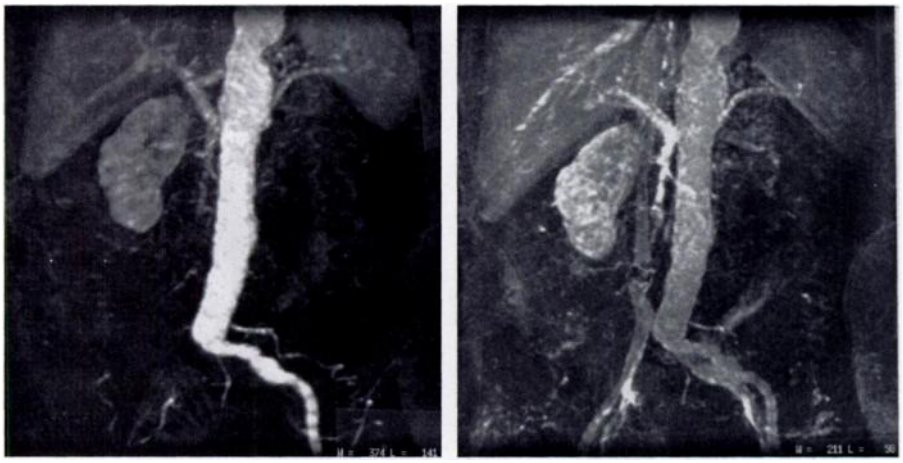

a. b.

Figure 11. Automated bolus-detection triggered MR angiographic images (6.7/1.9, 45° flip angle, 30-cm FOV, 38 3.5-mm-thick sections, 256 × 160 matrix, ±32-kHz bandwidth, one signal acquired in 41 seconds) in which the pulse sequence controller failed to detect a signal intensity increase; images correspond to the data in Figure 10. At a fail-safe limit of 45 seconds, the pulse sequence controller switched to automatic data-acquisition mode; thus, a diagnostically useful image was acquired. **(a)** Image shows clearly occlusion of the right iliac artery with substantial signal intensity enhancement in the arterial phase and little signal intensity enhancement in the venous phase. This can be compared to **b**, which was acquired immediately after the first image acquisition. **(b)** Delayed image shows clearly venous structures and diminished signal intensity in the arterial structures due to recirculation and dispersal of the contrast material. These images illustrate the usefulness of a fail-safe time limit.

suppression. The test bolus also limits the amount of contrast material that can be subsequently administered to the patient. This is an important consideration, because, in some parts of the world, the prohibitive cost of contrast material limits the use to a single 15-mL dose.

An alternative technique is that proposed by Mistretta and colleagues (11,12), in which a series of 3D volume images are collected over time, with the center of k space sampled more frequently than the other parts of k space; this is similar to keyhole imaging (13). With this technique, there is very little chance of missing the arrival of the contrast material bolus, because a 3D volume image is produced every 5–10 seconds by using a keyhole or sparse k-space acquisition. However, the patient is required to maintain a breath hold from the start of imaging for 30–40 seconds, because no indication is given about the arrival of the contrast material bolus.

All images are reconstructed, after appropriate filling in of missing k-space views, and the multiphase 3D images are reviewed to select that frame in time with maximal signal intensity in the arterial phase. Although this technique allows some time-based subtraction, similar to conventional digital subtraction angiography, it has severe image postprocessing and reconstruction demands. In addition, the patient has to maintain an effective breath hold throughout imaging so as to not generate motion-related artifacts in the subsequent images. These considerations preclude the performance of contrast material infusion MR angiography by MR technicians or radiographers without the presence of a skilled clinician. Furthermore, the image quality of these studies will vary with the experience of the clinician who supervises the imaging.

The proposed technique described in this article uses a pulse sequence with some automated intelligence. The robustness of an automated bolus-detection image is only as good as the placement of the tracking volume. If the volume is prescribed incorrectly or if the patient moves between the time a scout image is acquired and the start of the procedure, the pulse sequence controller is unable to detect any signal intensity amplitude increase. Subsequently, the trigger criteria are not met (as shown in Figure 10). If not for the fail-safe time limit, the tracking sequence would loop forever. The prescribed maximum tracking time of 30–50 seconds still allows acquisition of a clinically useful image with some signal intensity enhancement in the venous phase of circulation (Fig 11a). If we assume that the contrast material bolus is administered at the start of the tracking segment and a 15–20-second mean transit time, the fail-safe limit has delayed the start of data acquisition by only 20–30 seconds. Even with this delay, there is still signal intensity enhancement in the arterial vasculature sufficient for a clinical diagnosis. The worst-case scenario would be a result similar to that of a suboptimal, manually timed contrast-enhanced MR angiographic procedure.

The size of the tracking volume is another important consideration. Because a threshold criterion is a percentage of the increase in the detected signal intensity, a larger volume will have a larger fraction of (initially) nonenhanc-

ing stationary tissue. The higher the signal intensity in the nonenhancing background, the less sensitive the detection technique. Ideally, a combination of optimal tracking volume placement and adjustment of tracking volume size ensures optimal sensitivity to the contrast material bolus.

Although the proposed technique removes the variability of operator-dependent timing, the one element of operator dependency, that of tracking-volume placement and size adjustment, remains. An additional consideration is the position of the tracking volume relative to the imaging volume. Most MR imaging systems incorporate some postprocessing to correct for geometric distortion caused by gradient nonlinearities at the extremes of a large FOV. These gradient nonlinearities tend to distort the size and shape of the tracking volume far from the magnet isocenter. A tracking volume placed over an intended structure far from the isocenter of the imaging volume will suffer from gradient nonlinearity effects. This may lead to either a smaller fraction of arterial blood within the tracking volume or even missing the target structure altogether. With the graphic prescription capabilities available on our MR imager, the tracking volume can be placed as close to the isocenter (within or immediately adjacent to the imaging volume) as possible, which improves the tracking and detection sensitivity.

The proposed technique has many similarities to navigator echo techniques for reducing the effects of respiratory motion (14–16). However, rather than monitoring positional changes of a reference structure, the proposed technique monitors signal intensity changes within a reference structure. Both techniques use some real-time interaction between the pulse sequence controller and a separate processor that interprets the tracking or navigator MR signal intensity. In addition, the proposed technique has been used with a power infusion system.

A method that removes the guesswork in contrast material infusion timing for MR angiography has been demonstrated. The algorithm can successfully be used to detect the arterial phase of a contrast material bolus, provided the signal intensity enhancement is above the baseline noise due to respiratory motion. This method may also be useful for optimizing bolus timing in other MR studies that involve imaging during the arterial phase of contrast material infusion. ■

Acknowledgments: The authors thank James Kohli, MS, Rebecca McCann-Eggert, MS, Bo Pettersson, MS, and Kevin Kreger, MS, for their assistance with this project.

References

1. Lin W, Haacke EM, Smith AS, Clampitt ME. Gadolinium-enhanced high resolution MR angiography with adaptive vessel tracking: preliminary results in the intracranial circulation. JMRI 1992; 2:277–284.
2. Creasy JL, Price RR, Presby T, Goins D, Partain CL, Kessler RM. Gadolinium-enhanced MR angiography. Radiology 1990; 175:280–283.
3. Chakeres DW, Schmalbrock P, Brogan M, Yuan C, Cohen L. Normal venous anatomy of the brain: demonstration with gadopentetate dimeglumine in enhanced 3D MR angiography. AJNR 1990; 11:1107–1118.
4. Marchal G, Michiels J, Bosmans H, Van-Hecke P. Contrast enhanced MRA of the brain. J Comput Assist Tomogr 1992; 16: 25–29.
5. Losef SV, Rajan SS, Patt RH, et al. Gadolinium-enhanced magnitude contrast MR angiography of the popliteal and tibial arteries. Radiology 1992; 184:349–355.
6. Prince MR, Yucel EK, Kaufman JA, Harrison DC, Geller SC. Dynamic gadolinium-enhanced three-dimensional abdominal MR arteriography. JMRI 1993; 3:877–881.
7. Kanal E, Talagala SL, Applegate GR, Rubin RA, Foo TKF. Fast 3D TOF MRA with timed contrast injection (abstr). Radiology 1991; 181(P):119.
8. Talagala SL, Jungreis CA, Kanal E, et al. Fast three-dimensional time-of-flight MR angiography of the intracranial vasculature. JMRI 1995; 5:317–323.
9. Prince MR, Bass JC, Gabriel H, Londy FJ, Chenevert TL. Breath-held 3D gadolinium-enhanced renal artery MRA (abstr). In: Proceedings of the Third Meeting of the International Society for Magnetic Resonance in Medicine. Berkeley, Calif: International Society for Magnetic Resonance in Medicine, 1995; 539.
10. Holsinger AE, Riederer SJ. The importance of phase encoding order in ultrashort TR snapshot MR imaging. Magn Reson Med 1990; 16:481–488.
11. Mistretta CA, Grist TM, Frayne R, Korosec FR, Polzin JA. Simulation of a breath-hold method for time resolved 3D contrast imaging (abstr). In: Proceedings of the Fourth Meeting of the International Society for Magnetic Resonance in Medicine. Berkeley, Calif: International Society for Magnetic Resonance in Medicine, 1996; 1498.
12. Korosec FR, Grist TM, Frayne R, Polzin JA, Mistretta CA. Time-resolved contrast-enhanced 3D MR angiography. In: Proceedings of the Fourth Meeting of the International Society for Magnetic Resonance in Medicine. Berkeley, Calif: International Society for Magnetic Resonance in Medicine, 1996; 238.
13. van Vaals JJ, Brummer ME, Dixon WT, et al. Keyhole method for accelerating imaging of contrast uptake. JMRI 1993; 3:671–675.
14. Korin HW, Farzaneh F, Wright RC, Riederer SJ. Compensation for effects of linear motion in MR imaging. Magn Reson Med 1989; 12:99–113.
15. Korin HW, Felmlee JP, Ehman RL, Riederer SJ. Adaptive technique for three-dimensional MR imaging of moving structures. Radiology 1990; 177:217–221.
16. Fu ZW, Wang Y, Grimm RC, et al. Orbital navigator echoes for motion measurements in magnetic resonance imaging. Magn Reson Med 1995; 34:746–753.